# Supporting Information

## An Epidermis-Like Hierarchical Smart Coating with a Hardness of Tooth Enamel

Xiaodong Qi,[1] Dan Zhang,[2] Zhongbao Ma,[1] Wenxin Cao,[3] Ying Hou,[1] Jiaqi Zhu,[3] Yang Gan[2] and Ming Yang[1,*]

[1]Key Laboratory of Microsystems and Micronanostructures Manufacturing, [2]School of chemistry and Chemical Engineering, [3]Center for Composite Materials and Structures, Harbin Institute of Technology, 2 Yikuang Street, Harbin 150080, P.R. China

### A List of Figures and Tables

**Figure S12.** Optical and SEM images of a) $(PVA_{145k}/TA)_{50}@(PVA_{145k}\text{-}GO/TA)_{5}$, b) $(PVA_{145k}/TA)_{50}@(PVA_{145k}\text{-}GO/TA)_{8}$ c) $(PVA_{145k}/TA)_{50}@(PVA_{145k}\text{-}GO/TA)_{12}$ and d) $(PVA_{145k}/TA)_{50}@(PVA_{145k}\text{-}GO/TA)_{20}$ with a 50 μm wide cut throughout the film before and after immersion in water for 30 min.

**Figure S13.** Optical and SEM images of a) $(PVA_{47k}/TA)_{30}$, b) $(PVA_{47k}/TA)_{50}$, c) $(PVA_{47k}/TA)_{80}$, d) $(PVA_{145k}/TA)_{30}$, e) $(PVA_{145k}/TA)_{50}$ and f) $(PVA_{145k}/TA)_{80}$ with a 50 μm wide cut throughout the film before and after immersion in water for 30 min.

**Figure S14** Optical and SEM images of a) $(PVA_{47k}\text{-}GO/TA)_{10}$, b) $(PVA_{47k}\text{-}GO/TA)_{50}$, c) $(PVA_{47k}\text{-}GO/TA)_{80}$, d) $(PVA_{145k}\text{-}GO/TA)_{10}$, e) $(PVA_{145k}\text{-}GO/TA)_{50}$ and f) $(PVA_{145k}\text{-}GO/TA)_{80}$ with a 50 μm wide cut throughout the film before and after immersion in water for 30 min.

**Figure S15.** a) Surface and b) Cross-sectional SEM images of $(PVA_{47k}/TA)_{50}$ coatings with a 50 μm wide cut through the film before and after immersion in water for different lengths of time.

**Figure S16.** a) Surface and b) Cross-sectional SEM images of $(PVA_{47k}\text{-}GO/TA)_{10}$ coatings with a 50 μm wide cut through the film before and after immersion in water for different lengths of time.

**Figure S17.** A side view of the self-healing process on an e-LBL film with a thickness of *h* and a width of *w* (not shown in this schematic drawing). The white rectangular region denotes the crack with a width of *z*. $c_1$, $c_2$ and $c_3$ are polymer concentrations in the film, crack area and solution, respectively. $k_{in}$ and $k_{out}$ are the mass transfer coefficients into and out of the crack area.

**Figure S18.** Cross-sectional fluorescent optical images of a) $(PVA_{145k}/TA)_{50}$ and $(PVA_{145k}\text{-}GO/TA)_{10}$ after their immersion into $PVA_{145k}$-c solutions for 5 min and 1 min, respectively. The immersion time is chosen to avoid complete diffusion across the film so that the diffusion rate can be calculated.

**Figure S19**. TGA results for GO, $(PVA_{145k}/TA)_{50}$, $(PVA_{47k}/TA)_{50}$, $(PVA_{145k}\text{-}GO/TA)_{10}$ and $(PVA_{47k}\text{-}GO/TA)_{10}$.

**Figure S20.** IR spectra of $PVA_{47k}$, TA and the solutions after immersion of $(PVA_{47k}/TA)_{50}$, $(PVA_{47k}/TA)_{50}@(PVA_{47k}\text{-}GO/TA)_{5}$, $(PVA_{47k}/TA)_{50}@(PVA_{47k}\text{-}GO/TA)_{10}$, $(PVA_{47k}/TA)_{50}@(PVA_{47k}\text{-}GO/TA)_{20}$, and $(PVA_{47k}\text{-}GO/TA)_{10}$ into 50 mL DI water for 30 min.

**Figure S21.** Surface fluorescent optical images of $(PVA_{145k}/TA)_{50}(PVA_{145k}\text{-}c/TA)$ after the additional depositions of a) 0, b) 5, c) 10 and d) 20 bilayers of $PVA_{145k}\text{-}GO/TA$ and e) 5 and f) 10 bilayers of $PVA_{145k}/TA$.

**Figure S22.** The plotting of TA absorbance against different lengths of immersion time in 50 mL water for a) $(PVA_{47k}\text{-}GO/TA)_{10}$ and $(PVA_{47k}/TA)_{50}$ with different bilayers of $(PVA_{47k}\text{-}GO/TA)$ and b) $(PVA_{145k}\text{-}GO/TA)_{10}$ and $(PVA_{145k}/TA)_{50}$ with different bilayers of $(PVA_{145k}\text{-}GO/TA)$ on the top.

**Figure S23.** a,b) Cross-sectional and c,d) surface fluorescent optical images of a,c) $(PVA_{47k}\text{-}c\text{-}GO/TA)(PVA_{47k}\text{-}GO/TA)_{9}$ and b,d) $(PVA_{47k}\text{-}c\text{-}GO/TA)(PVA_{47k}\text{-}GO/TA)_{19}$.

The dotted surface fluorescence may be due to the high roughness of l-LBL film growing on glass substrates. The insets in a and b indicate the thickness of the film.

**Figure S24.** a,b) Cross-sectional and c,d) surface fluorescent optical images of a,c) $(PVA_{145k}\text{-c-GO/TA})(PVA_{145k}\text{-GO/TA})_9$ and b,d) $(PVA_{145k}\text{-c-GO/TA})(PVA_{145k}\text{-GO/TA})_{19}$. The dotted surface fluorescence may be due to the high roughness of l-LBL film growing on glass substrates. The insets in a and b indicate the thickness of the film.

**Figure S25.** SEM images of a) $(PVA_{47k}/TA)_{50}@(PVA_{47k}\text{-GO/TA})_{20}$ and b) $(PVA_{145k}/TA)_{50}@(PVA_{145k}\text{-GO/TA})_{20}$.

**Figure S26.** Optical and SEM images of a) $(PEG/TA)_{50}$, b) $(PEG\text{-GO/TA})_{10}$ and c) $(PEG/TA)_{50}@(PEG\text{-GO/TA})_{10}$ coatings with a 50 μm wide cut through the film before and after immersion in water for different lengths of time.

**Figure S27.** Load-displacement curves for a) $(PVA_{145k}/TA)_{50}$, $(PVA_{145k}\text{-GO/TA})_{10}$, $(PVA_{145k}/TA)_{50}@(PVA_{145k}\text{-GO/TA})_{10}$ and b) the crack area after self-healing for $(PVA_{47k}/TA)_{50}@(PVA_{47k}\text{-GO/TA})_{10}$ and $(PVA_{145k}/TA)_{50}@(PVA_{145k}\text{-GO/TA})_{10}$.

**Table S1.** A summary of modulus and hardness for different multilayers consisting of $PVA_{145k}$ obtained from nanoindentation.

**Table S2.** A summary of modulus and hardness for hybrid films before and after self-healing obtained from nanoindentation.

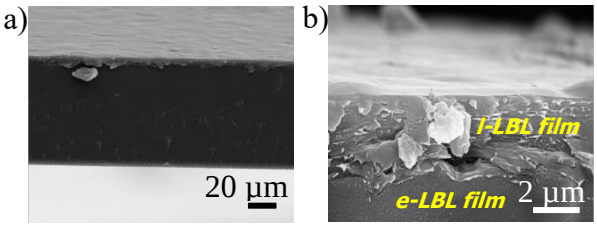


**Figure S1.** Cross-sectional SEM images of $(PVA_{145k}/TA)_{50}$@$(PVA_{145k}$-GO/TA$)_{10}$.

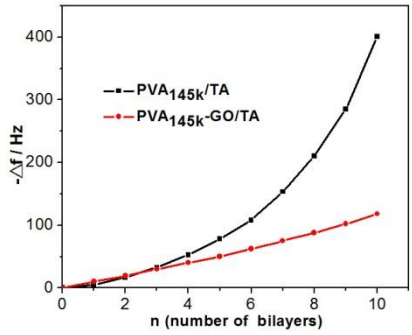


**Figure S2.** QCM results for the growth of first ten bilayers of $PVA_{145k}$/TA and $PVA_{145k}$-GO/TA.

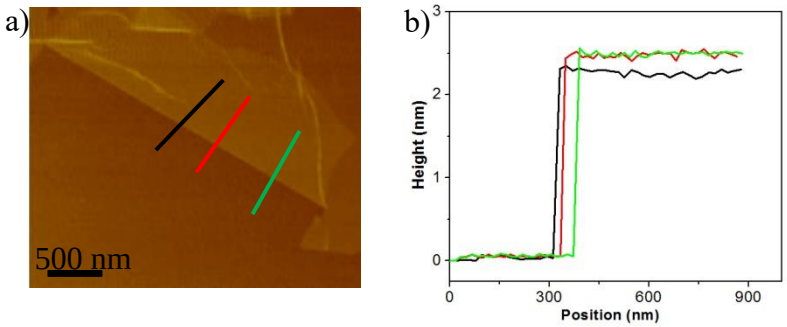


**Figure S3.** a) The AFM image and b) thickness profiles of GO.

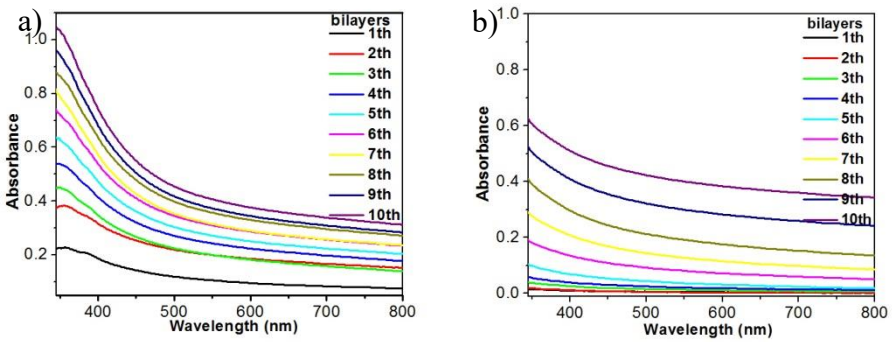


**Figure S4.** Compilation of UV-vis spectra of $PVA_{47k}$-GO/TA during the growth of first 10 bilayers on a) $(PVA_{47k}/TA)_{50}$ and b) glass substrates.

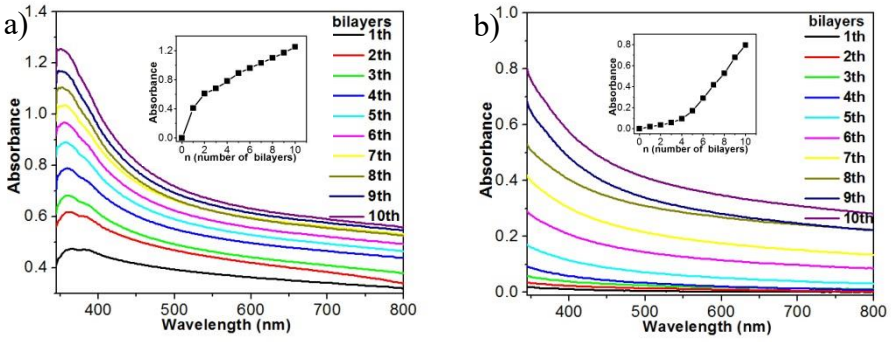


**Figure S5.** Compilation of UV-vis spectra of $PVA_{145k}$-GO/TA during the growth of the first 10 bilayers on a) $(PVA_{145k}/TA)_{50}$ and b) glass substrates. The insets are the plotting of absorbance at 345 nm against the number of bilayers.

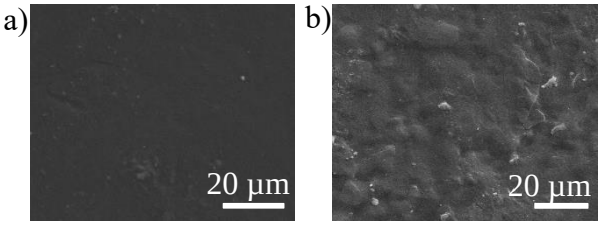


**Figure S6.** SEM images of $(PVA_{145k}$-GO/TA$)_{10}$ growing on a) $(PVA_{145k}/TA)_{50}$ and b) glass substrates.

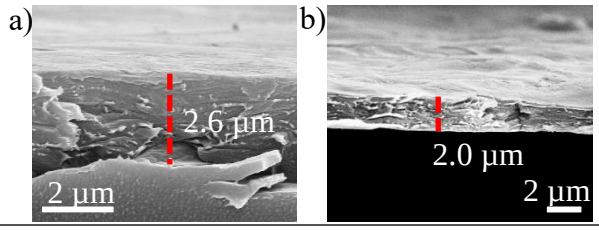


**Figure S7.** Cross-sectional SEM images of a) $(PVA_{145k}/TA)_{50}@(PVA_{145k}\text{-}GO/TA)_{10}$ and b) $(PVA_{145k}\text{-}GO/TA)_{10}$ on glass substrates.

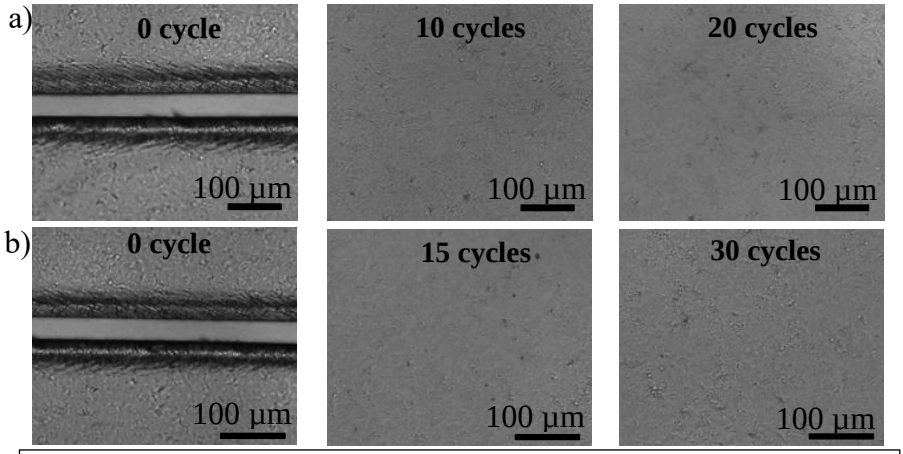


**Figure S8.** Optical images of a) $(PVA_{47k}/TA)_{50}@(PVA_{47k}\text{-}GO/TA)_{10}$ and b) $(PVA_{47k}/TA)_{80}@(PVA_{47k}\text{-}GO/TA)_{10}$ with different scratch/healing cycles.

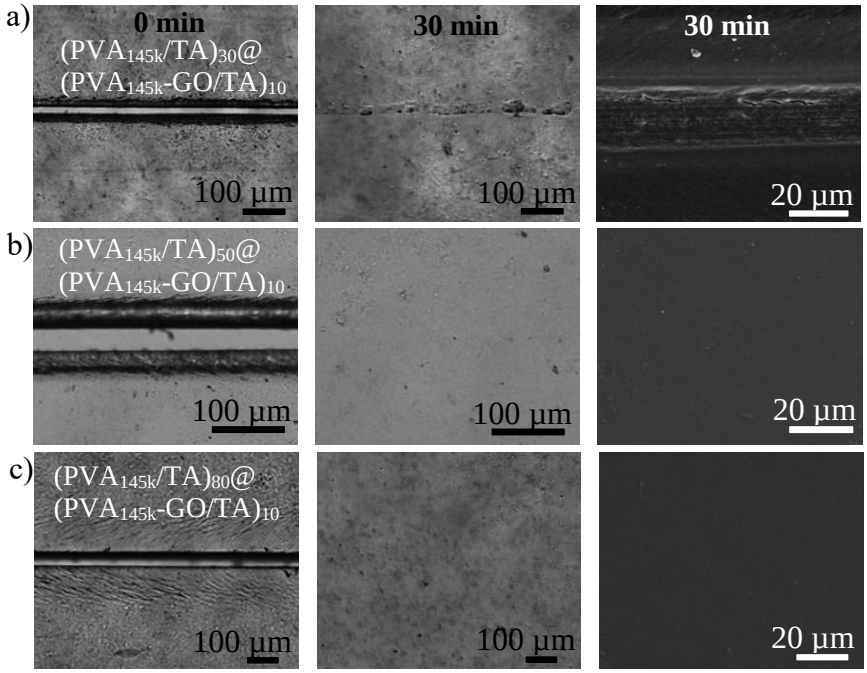


**Figure S9.** Optical and SEM images of a) $(PVA_{145k}/TA)_{30}@(PVA_{145k}\text{-}GO/TA)_{10}$, b) $(PVA_{145k}/TA)_{50}@(PVA_{145k}\text{-}GO/TA)_{10}$ and c) $(PVA_{145k}/TA)_{80}@(PVA_{145k}\text{-}GO/TA)_{10}$ with a 50 µm wide cut throughout the film before and after immersion in water for 30 min.

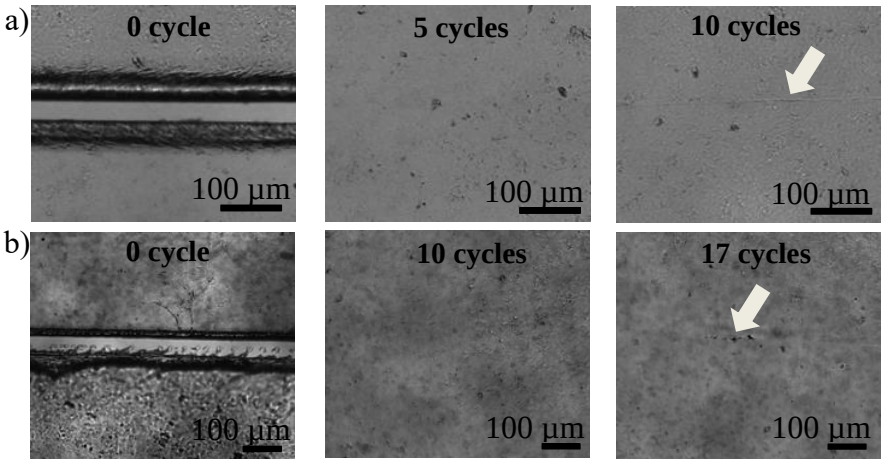


**Figure S10.** Optical images of a) $(PVA_{145k}/TA)_{50}@(PVA_{145k}\text{-}GO/TA)_{10}$ and b) $(PVA_{145k}/TA)_{80}@(PVA_{145k}\text{-}GO/TA)_{10}$ with different cutting-healing cycles. The insets indicate the emergence of unrecovered surface scratch.

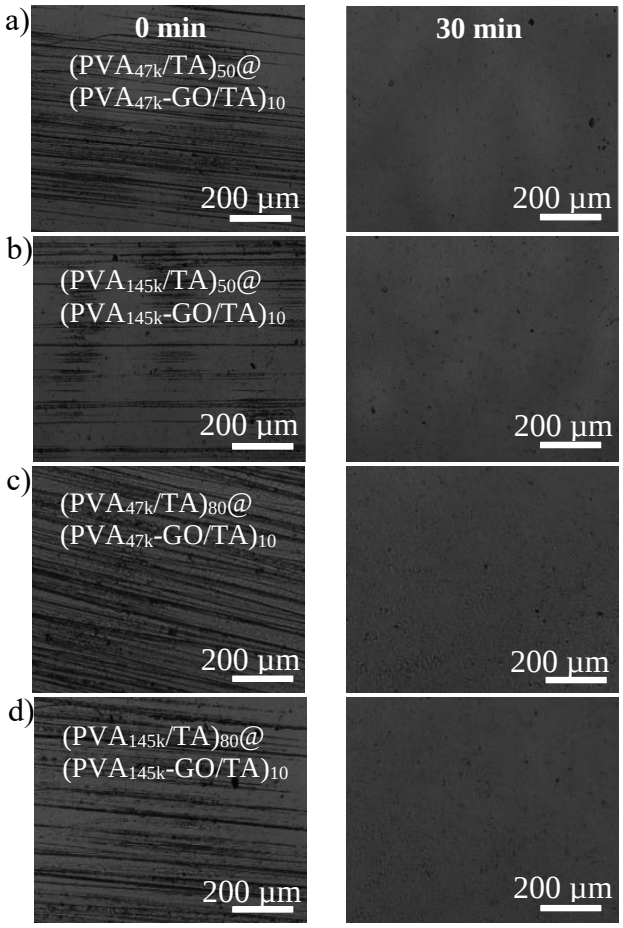


**Figure S11.** Optical images of a) $(PVA_{47k}/TA)_{50}@(PVA_{47k}\text{-}GO/TA)_{10}$, b) $(PVA_{145k}/TA)_{50}@(PVA_{145k}\text{-}GO/TA)_{10}$, c) $(PVA_{47k}/TA)_{80}@(PVA_{47k}\text{-}GO/TA)_{10}$, and d) $(PVA_{145k}/TA)_{80}@(PVA_{145k}\text{-}GO/TA)_{10}$ scratched by a sand paper before and after immersion in water for 30 min.

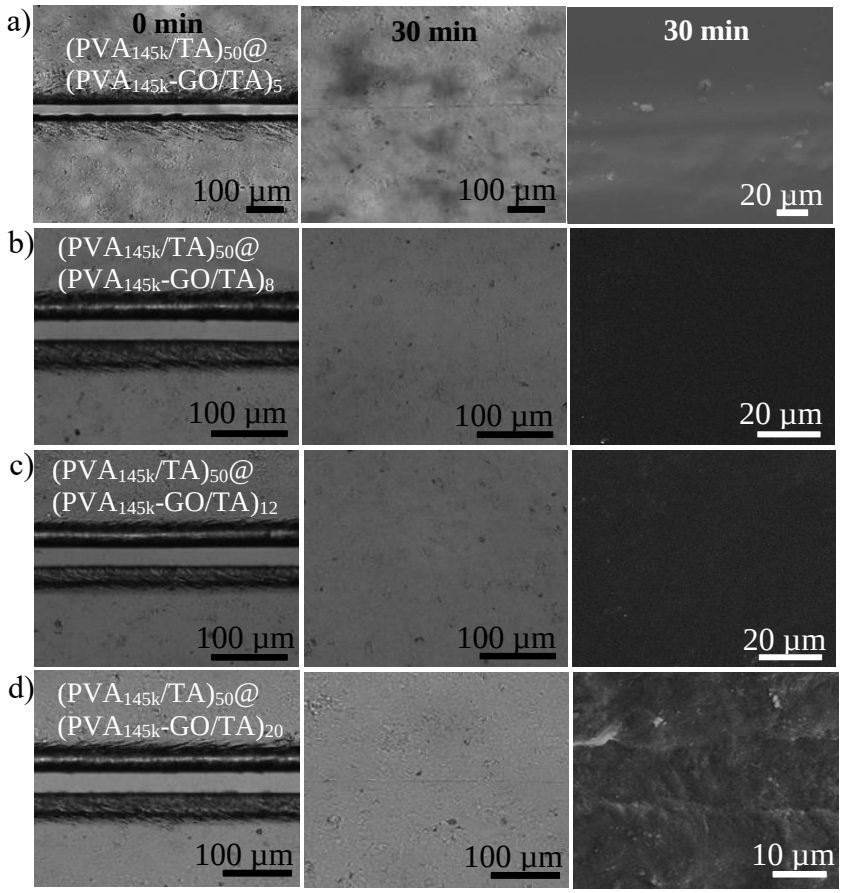


**Figure S12.** Optical and SEM images of a) $(PVA_{145k}/TA)_{50}@(PVA_{145k}\text{-}GO/TA)_5$, b) $(PVA_{145k}/TA)_{50}@(PVA_{145k}\text{-}GO/TA)_8$ c) $(PVA_{145k}/TA)_{50}@(PVA_{145k}\text{-}GO/TA)_{12}$ and d) $(PVA_{145k}/TA)_{50}@(PVA_{145k}\text{-}GO/TA)_{20}$ with a 50 µm wide cut throughout the film before and after immersion in water for 30 min.

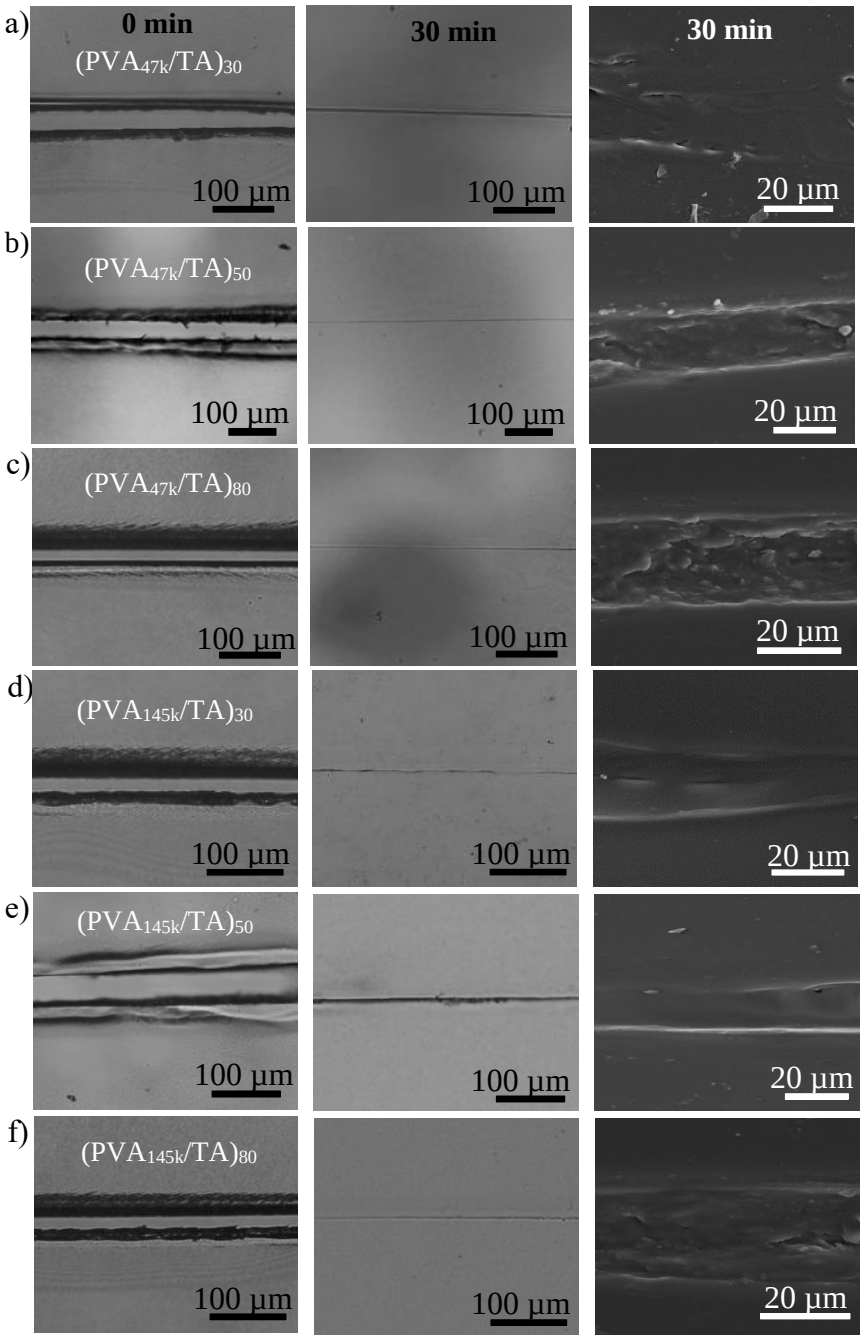


**Figure S13.** Optical and SEM images of a) $(PVA_{47k}/TA)_{30}$, b) $(PVA_{47k}/TA)_{50}$, c) $(PVA_{47k}/TA)_{80}$, d) $(PVA_{145k}/TA)_{30}$, e) $(PVA_{145k}/TA)_{50}$ and f) $(PVA_{145k}/TA)_{80}$ with a 50 µm wide cut throughout the film before and after immersion in water for 30 min.

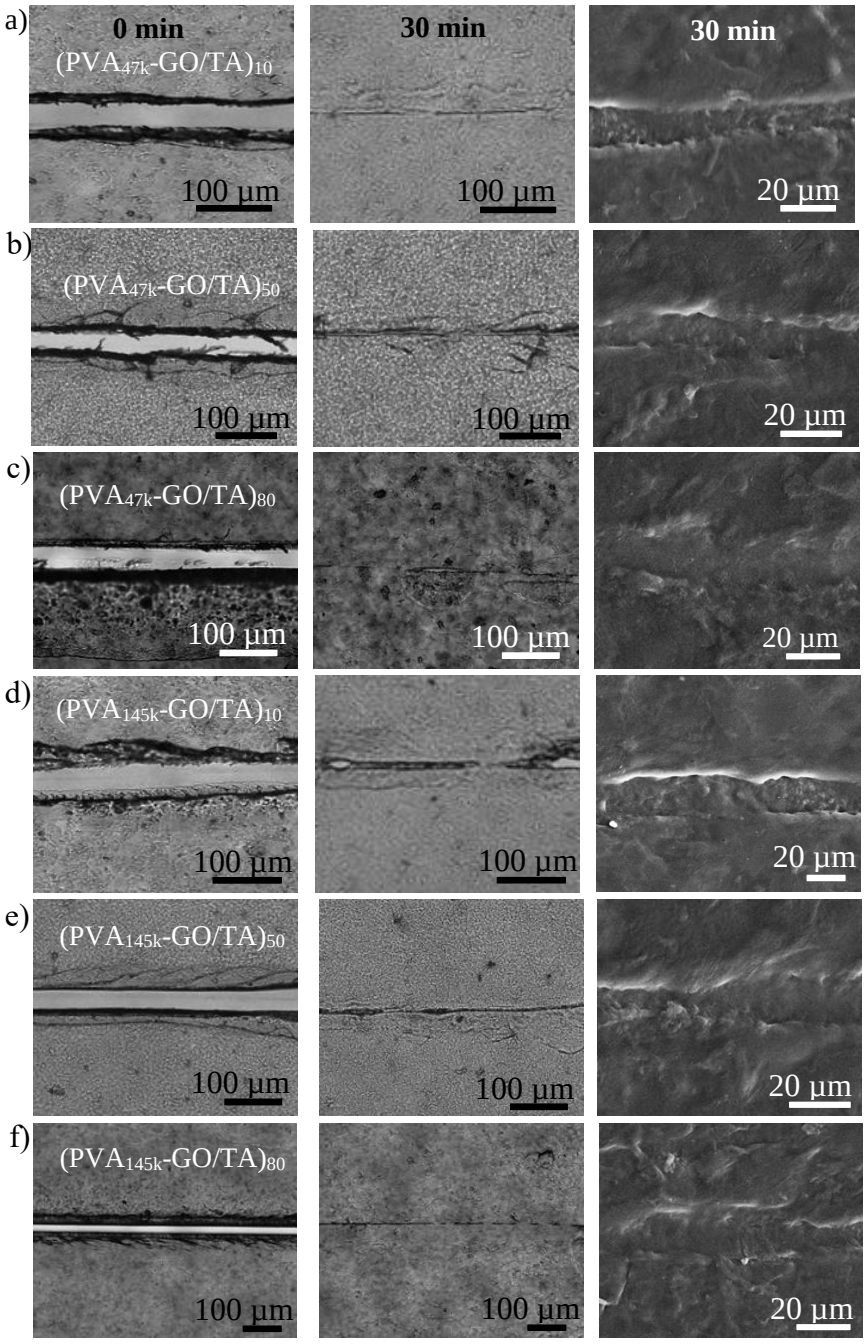


**Figure S14** Optical and SEM images of a) $(PVA_{47k}\text{-}GO/TA)_{10}$, b) $(PVA_{47k}\text{-}GO/TA)_{50}$, c) $(PVA_{47k}\text{-}GO/TA)_{80}$, d) $(PVA_{145k}\text{-}GO/TA)_{10}$, e) $(PVA_{145k}\text{-}GO/TA)_{50}$ and f) $(PVA_{145k}\text{-}GO/TA)_{80}$ with a 50 µm wide cut throughout the film before and after immersion in water for 30 min.

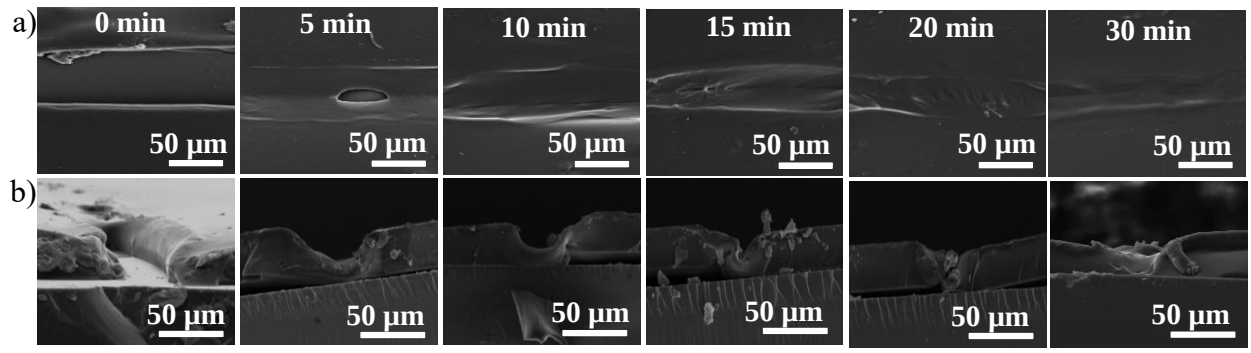


**Figure S15.** a) Surface and b) cross-sectional SEM images of $(PVA_{47k}/TA)_{50}$ with a 50 µm wide cut throughout the film before and after immersion in water for different lengths of time.

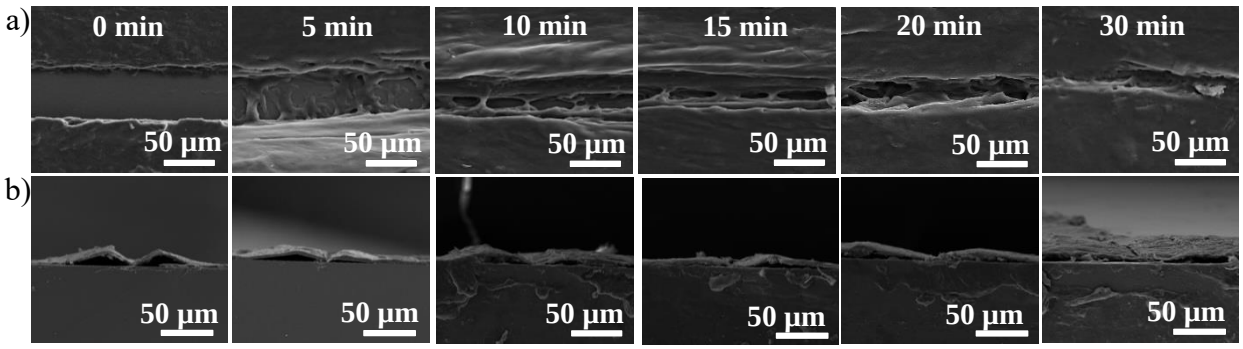


**Figure S16.** a) Surface and b) cross-sectional SEM images of $(PVA_{47k}\text{-}GO/TA)_{10}$ with a 50 µm wide cut throughout the film before and after immersion in water for different lengths of time.

**Details about the development of theoretical model**: The flux (*J*) into and out of the crack area (Figure S17) can be expressed as

$$J_{in} = Ak_{in}(c_1 - c_2) = hwk_{in}(c_1 - c_2) \quad (1)$$

$$J_{out} = A'k_{out}(c_2 - c_3) = zwk_{out}(c_2 - c_3) \quad (2)$$

where $k_{in}$ and $k_{out}$ are the mass transfer coefficients into and out of the crack with the cross-sectional areas of *A* and *A'*, respectively; *h* is the thickness of the film, *z* is the length of the crack and *w* is the width of the film; $c_1$, $c_2$ and $c_3$ are polymer concentrations in the film, crack area and solution, respectively.

We also have

$$V\frac{dc_2}{dt} = Ak_{in}(c_1 - c_2) - A'k_{out}(c_2 - c_3) \quad (3)$$

where $V$ is the volume of the crack part.

We use the initial condition ($t$ = 0; $c_2$ = 0) to integrate the mass balance which gives

$$c_2 = \frac{Ak_{in}c_1 + A'k_{out}c_3}{Ak_{in} + A'k_{out}}\left(1 - e^{-\left(\frac{Ak_{in}+A'k_{out}}{V}\right)t}\right) \quad (4)$$

Here $c_1$ can be regarded as a constant and $c_3$ can be essentially zero due to the large volume of the solution. Also consider that $k_{out}$ is much smaller than $k_{in}$ due to the interactions between PVA and TA, we have

$$c_2 = c_1\left(1 - e^{-\left(\frac{Ak_{in}}{V}\right)t}\right) \quad (5)$$

After a time of $t_e$, an equilibrium is established,

$$J_{in} = J_{out} \quad (6)$$

So

$$hwk_{in}(c_1 - c_2) = zwk_{out}(c_2 - c_3) \quad (7)$$

Combining (5) and (7) gives

$$hk_{in}e^{-\left(\frac{k_{in}A}{V}\right)t_e}c_1 = zk_{out}\left(1 - e^{-\left(\frac{k_{in}A}{V}\right)t_e}\right)c_1 \quad (8)$$

Then we have

$$e^{-\left(\frac{k_{in}A}{V}\right)t_e} = \frac{zk_{out}}{hk_{in} + zk_{out}} \quad (9)$$

According to (9), $t_e$ is in reverse proportion to $k_{out}$. On the other hand, suppose that after a time period ($t_r$), a complete repair can be achieved. According to (5), $t_r$ is mainly determined by and reversely proportional to $k_{in}$.

As at the equilibrium, no further accumulation in the crack area can be expected, to make a full recovery, it is necessary to have

$$t_r < t_e$$

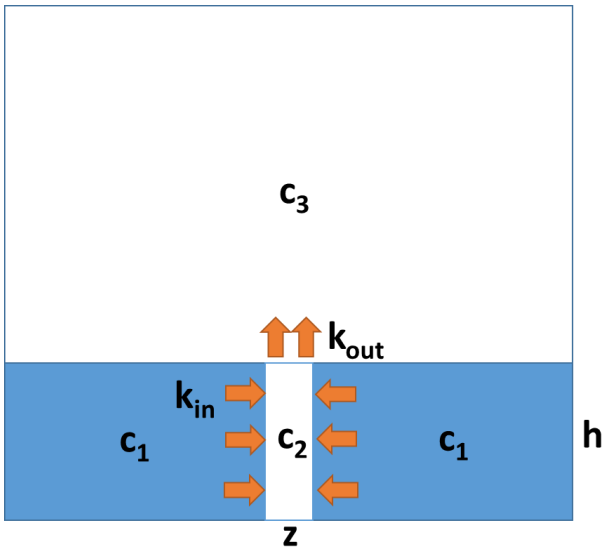


**Figure S17.** A side view of the self-healing process on an e-LBL film with a thickness of *h* and a width of *w* (not shown in this schematic drawing). The white rectangular region denotes the crack with a width of *z*. $c_1$, $c_2$ and $c_3$ are polymer concentrations in the film, crack area and solution, respectively. $k_{in}$ and $k_{out}$ are the mass transfer coefficients into and out of the crack area.

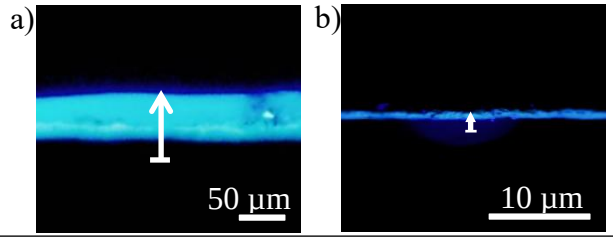


**Figure S18.** Cross-sectional fluorescent optical images of a) $(PVA_{145k}/TA)_{50}$ and $(PVA_{145k}\text{-}GO/TA)_{10}$ after their immersion into $PVA_{145k}$-c solutions for 5 min and 1 min, respectively. The immersion time is chosen to avoid complete diffusion across the film so that the diffusion rate can be calculated.

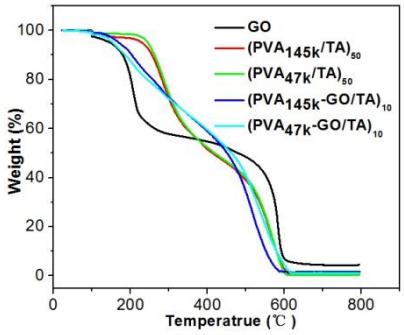


**Figure S19**. TGA results for GO, $(PVA_{145k}/TA)_{50}$, $(PVA_{47k}/TA)_{50}$, $(PVA_{145k}\text{-}GO/TA)_{10}$ and $(PVA_{47k}\text{-}GO/TA)_{10}$.

**The determination of GO contents in the film:** Thermogravimetric analysis (TGA) was used to calculate the contents of GO in l-LBL film (Figure S19). $(PVA/TA)_{50}$ can decompose completely when reaching 620 $^{o}$C under oxygen atmosphere, however, GO does not fully decompose at a temperature as high as 800 $^{o}$C. The above fact provides a simple method to calculate the percentage of GO in $(PVA\text{-}GO/TA)_{10}$. In Eq. 1, *a* and *b* are the remaining contents of GO and $(PVA\text{-}GO/TA)_{10}$ at 800 $^{o}$C, respectively; *x* is therefore the contents of GO in $(PVA\text{-}GO/TA)_{10}$.

$$ax = b \qquad (1)$$

According to Eq. 1, there are approximately 30 % and 35 % GO in $(PVA_{47k}\text{-}GO/TA)_{10}$ and $(PVA_{145k}\text{-}GO/TA)_{10}$, respectively.

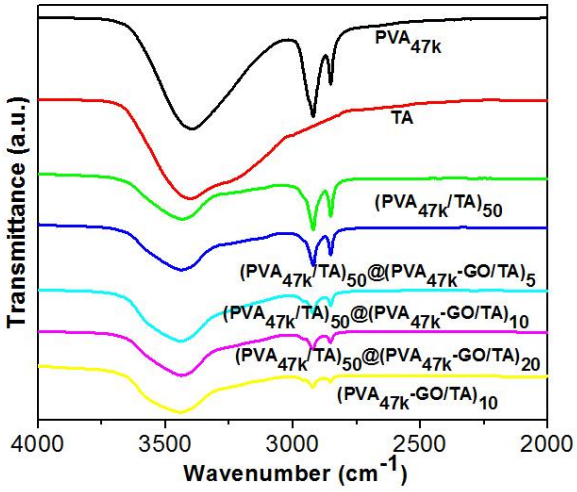


**Figure S20.** IR spectra of $PVA_{47k}$, TA and the solutions after immersion of $(PVA_{47k}/TA)_{50}$, $(PVA_{47k}/TA)_{50}@(PVA_{47k}\text{-}GO/TA)_{5}$, $(PVA_{47k}/TA)_{50}@(PVA_{47k}\text{-}GO/TA)_{10}$, $(PVA_{47k}/TA)_{50}@(PVA_{47k}\text{-}GO/TA)_{20}$, and $(PVA_{47k}\text{-}GO/TA)_{10}$ into 50 mL DI water for 30 min.

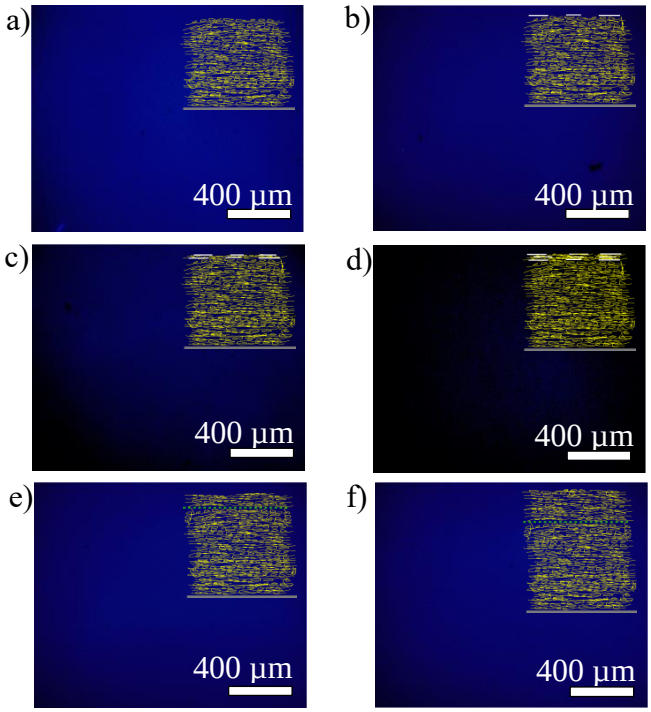


**Figure S21.** Surface fluorescent optical images of $(PVA_{145k}/TA)_{50}(PVA_{145k}\text{-c/TA})$ after the additional depositions of a) 0, b) 5, c) 10 and d) 20 bilayers of $PVA_{145k}$-GO/TA and e) 5 and f) 10 bilayers of $PVA_{145k}$/TA.

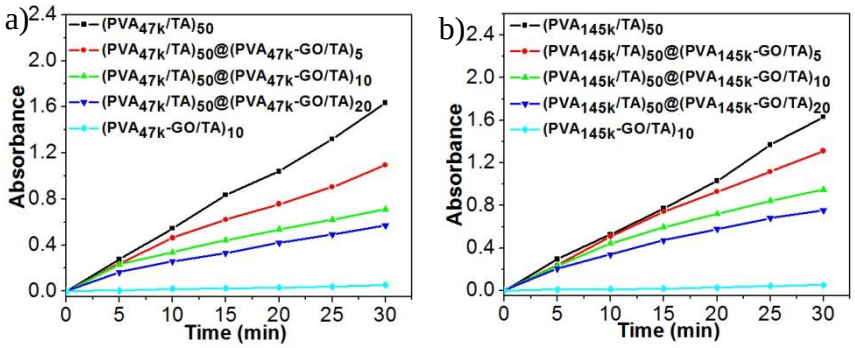


**Figure S22.** The plotting of TA absorbance against different lengths of immersion time in 50 mL water for a) $(PVA_{47k}\text{-GO/TA})_{10}$ and $(PVA_{47k}/TA)_{50}$ with different bilayers of $(PVA_{47k}\text{-GO/TA})$ and b) $(PVA_{145k}\text{-GO/TA})_{10}$ and $(PVA_{145k}/TA)_{50}$ with different bilayers of $(PVA_{145k}\text{-GO/TA})$ on the top.

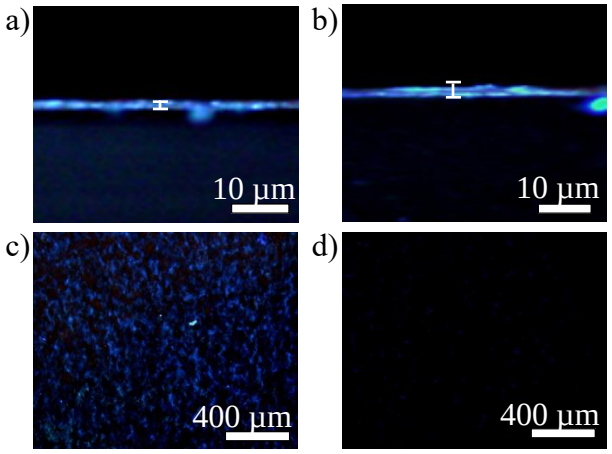


**Figure S23** a,b) Cross-sectional and c,d) surface fluorescent optical images of a,c) $(PVA_{47k}\text{-c-GO/TA})(PVA_{47k}\text{-GO/TA})_9$ and b,d) $(PVA_{47k}\text{-c-GO/TA})(PVA_{47k}\text{-GO/TA})_{19}$. The dotted surface fluorescence may be due to the high roughness of l-LBL film growing on glass substrates. The insets in a and b indicate the thickness of the film.

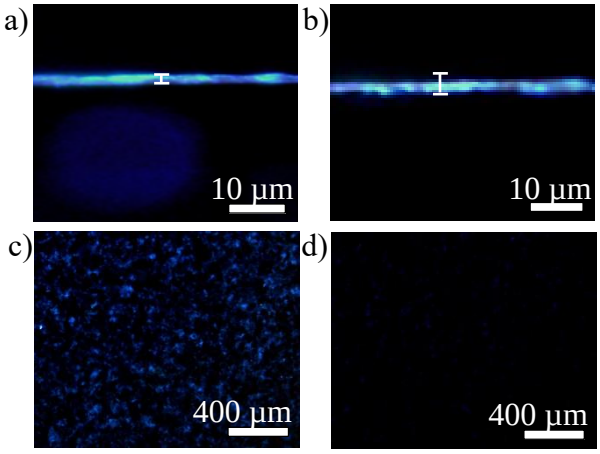


**Figure S24.** a,b) Cross-sectional and c,d) surface fluorescent optical images of a,c) $(PVA_{145k}\text{-c-GO/TA})(PVA_{145k}\text{-GO/TA})_9$ and b,d) $(PVA_{145k}\text{-c-GO/TA})(PVA_{145k}\text{-GO/TA})_{19}$. The dotted surface fluorescence may be due to the high roughness of l-LBL film growing on glass substrates. The insets in a and b indicate the thickness of the film.

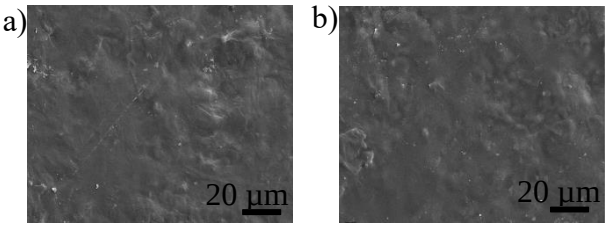


**Figure S25.** SEM images of a) $(PVA_{47k}/TA)_{50}@(PVA_{47k}\text{-GO/TA})_{20}$ and b) $(PVA_{145k}/TA)_{50}@(PVA_{145k}\text{-GO/TA})_{20}$.

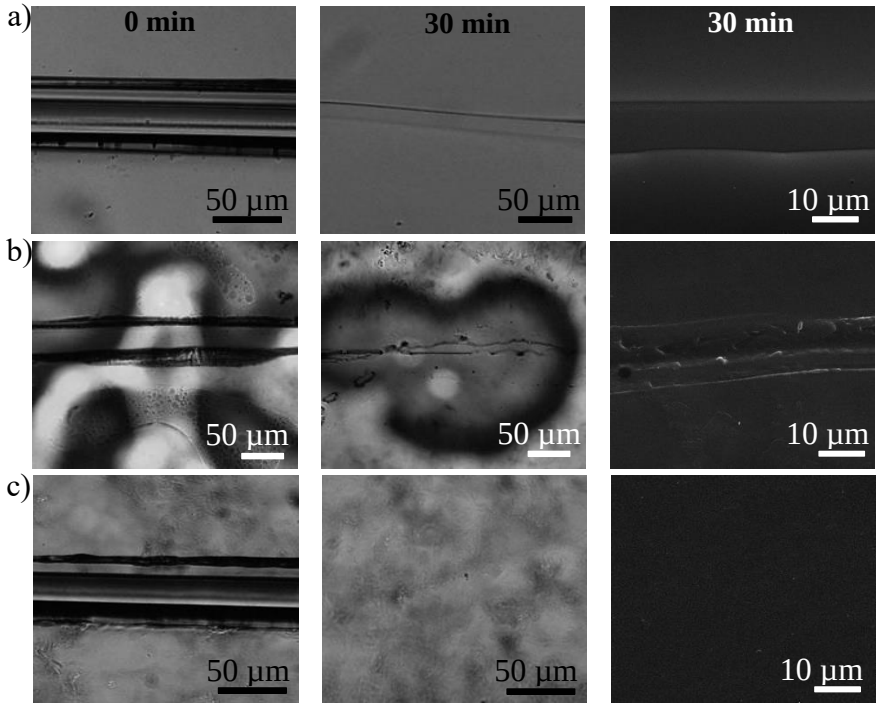


**Figure S26.** Optical and SEM images of a) $(PEG/TA)_{50}$, b) $(PEG\text{-}GO/TA)_{10}$ and c) $(PEG/TA)_{50}@(PEG\text{-}GO/TA)_{10}$ with a 50 µm wide cut throughout the film before and after immersion in water for 30 min.

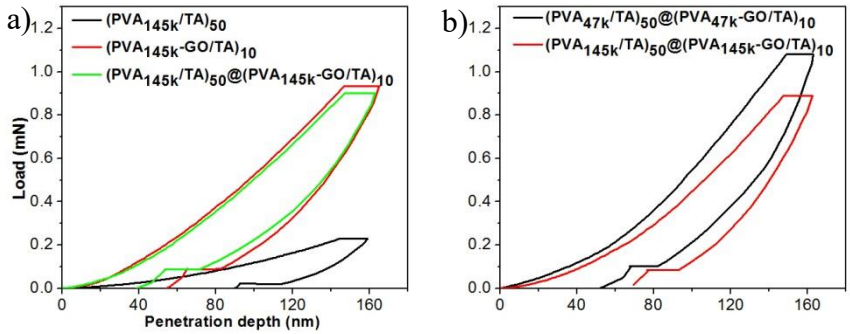


**Figure S27.** Load-displacement curves for a) $(PVA_{145k}/TA)_{50}$, $(PVA_{145k}\text{-}GO/TA)_{10}$, $(PVA_{145k}/TA)_{50}@(PVA_{145k}\text{-}GO/TA)_{10}$ and b) the crack area after self-healing for $(PVA_{47k}/TA)_{50}@(PVA_{47k}\text{-}GO/TA)_{10}$ and $(PVA_{145k}/TA)_{50}@(PVA_{145k}\text{-}GO/TA)_{10}$.

| Samples | Modulus *E* (GPa) | Hardness *H* (GPa) |
|---|---|---|
| $(PVA_{145k}/TA)_{50}$ | 8.7±0.1 | 0.44±0.02 |
| $(PVA_{145k}\text{-}GO/TA)_{10}$ | 26.7±0.4 | 2.18±0.11 |
| $(PVA_{145k}/TA)_{50}@(PVA_{145k}\text{-}GO/TA)_{10}$ | 25.1±2.2 | 2.11±0.22 |

**Table S1.** A summary of modulus and hardness for different multilayers consisting of $PVA_{145k}$ obtained from nanoindentation.

| Modes | Samples | Modulus *E* (GPa) | Hardness *H* (GPa) |
|---|---|---|---|
| Before self-healing | $(PVA_{47k}/TA)_{50}@(PVA_{47k}\text{-}GO/TA)_{10}$ | 31.4±1.8 | 2.27±0.09 |
| | $(PVA_{145k}/TA)_{50}@(PVA_{145k}\text{-}GO/TA)_{10}$ | 25.1±2.2 | 2.11±0.22 |
| After self-healing | $(PVA_{47k}/TA)_{50}@(PVA_{47k}\text{-}GO/TA)_{10}$ | 31.3±1.9 | 2.21±0.05 |
| | $(PVA_{145k}/TA)_{50}@(PVA_{145k}\text{-}GO/TA)_{10}$ | 24.3±0.8 | 2.09±0.26 |

**Table S2.** A summary of modulus and hardness for hybrid films before and after self-healing obtained from nanoindentation.